

A Multi-Layer ML–Econometric Pipeline for Forecasting Market Risk: Evidence from Crypto Liquidity Spillovers

Yimeng Qiu
LSEG
US

Feihuang Fang
LSEG
UK

Abstract

We test whether liquidity/volatility proxies of a small set of core cryptoassets exhibit spillovers that forecast *market-wide* risk. Our pipeline stacks three statistical layers (A: core LV↔core returns; B: PC(LV)↔PC(returns); C: vol-PCs→cross-sectional “volatility crowding”) and complements them with VAR IRF/FEVD [10, 17], HAR-X [8], and a leakage-safe ML protocol (time splits, early stopping, validation-only thresholding, SHAP). Using daily data from 2021 to 2025 (1462 × 74; latest artifacts under output/run_20250808_221301), we find significant Granger links across layers and moderate OOS performance. We report only the most probative figures (pipeline overview, Layer A heatmap, Layer C robustness, VAR FEVD, and a test-set PR curve) while providing full CSV/PNGs in the artifact directory.

1 Introduction

Liquidity and volatility co-move across assets, producing spillovers during stress periods [2, 3, 7, 9]. We ask whether a compact set of *core* coins contains enough information to forecast *market-wide* risk. We operationalize a three-layer chain of evidence:

- **Layer A:** core liquidity/volatility (LV) ↔ core returns.
- **Layer B:** principal components of LV ↔ principal components of returns.
- **Layer C:** volatility PCs → a cross-sectional “volatility crowding” target.

We then estimate compact VARs for IRF/FEVD interpretation, fit HAR-X with HAC errors, and train early-stopped XGBoost models on chronological splits. Contributions: (i) a cross-sectional L2 “crowding” target aligned to vol-PCs; (ii) a leakage-aware forecasting protocol; (iii) reproducible artifacts (logs/CSVs/figures) under output/run_20250808_221301.

2 Related Work

We build on classical tools for dynamic dependence and volatility modeling. Granger causality and VARs provide the workhorse framework for testing predictive links and impulse propagation [10, 17]. Our liquidity/volatility proxies follow standard microstructure and range-based measures—Amihud illiquidity and Parkinson high/low volatility—and are complemented by GARCH-type variation [2, 4, 15]. To capture long-memory structure, we adopt HAR-X with HAC inference [8, 14]. For forecasting and interpretability, we employ gradient-boosted trees and SHAP explanations [6, 13]. Relative to this literature, we connect *core-coin* microstructure signals to a *market-wide* cross-sectional “volatility crowding” target via a multi-layer causality chain, and we evaluate predictability under a leakage-aware protocol (see Figure 1).

3 Method

3.1 Data and Preprocessing

We assemble daily prices/volume from public aggregators (Yahoo Finance, CoinMarketCap) and build an engineered panel with 1462 × 74 entries (latest run under output/run_20250808_221301). The core coin set is ETH, BTC, YFI, DOT, XEM, BNB, ARK. From these, we compute log-returns, Amihud illiquidity [2], turnover, and two volatility proxies (GARCH(1,1), Parkinson high/low). For interpretability, we retain key raw indicators for major cores and form principal components for the rest; the returns PCs keep $k=3$ explaining 85.26% cumulative variance. To attenuate mechanical leverage effects, for each core we regress volatility proxies on its own return and keep residuals (residual vol/turnover columns). For comparison, we also construct legacy market targets based on 14-day realized volatility and its rolling-standardized variant (market_rv14, market_rv14_rs); all artifacts/CSVs are exported under output/run_20250808_221301.

Core-coin selection. We endogenously select “core” coins by constructing a directed Granger network on standardized log-returns and keeping the strongest *senders* by PageRank [5]. Specifically,

$$i \rightarrow j \text{ iff } \min_{\ell=1,\dots,5} p_{i \rightarrow j}(\ell) < 0.05,$$

and we rank nodes by PageRank on G^\top (damping $\alpha=0.85$), taking the top- N and enforcing a small whitelist {BTC, ETH, BNB} for coverage. The latest run yields ETH, BTC, YFI, DOT, XEM, BNB, ARK. From these, we compute log-returns, Amihud illiquidity, turnover, and two volatility proxies (GARCH(1,1), Parkinson high/low). For interpretability, we retain key raw indicators for major cores and form principal components for the rest; the returns PCs keep $k=3$ explaining 85.26% cumulative variance. To attenuate mechanical leverage effects, for each core we regress volatility proxies on its own return and keep residuals. We also construct legacy targets (market_rv14, market_rv14_rs); all artifacts/CSVs are under output/run_20250808_221301.

3.2 Targets and Factors

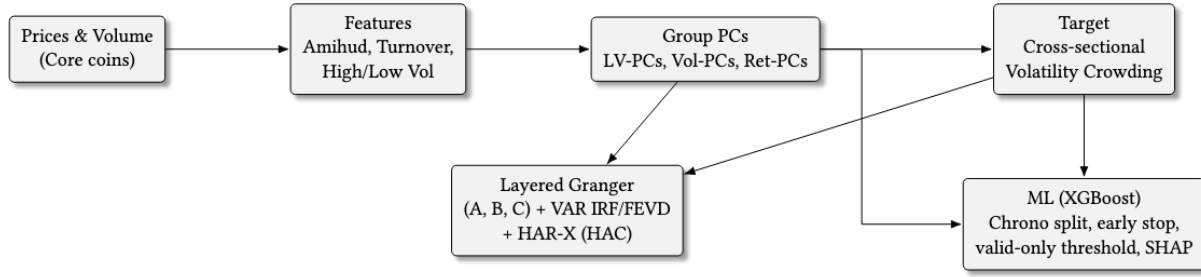
From daily data on core coins (e.g., BTC, ETH, BNB, YFI, ...), we compute log-returns, Amihud illiquidity, turnover, and high/low-based volatility. For each group, we form PCs. The *volatility crowding* target is

$$\text{mkt_xsec_vol_l2}(t) = \sqrt{\frac{1}{K} \sum_{k=1}^K z_k(t)^2}, \quad z_k(t) = \frac{\text{PC}_k^{(\text{vol})}(t) - \mu_k}{\sigma_k},$$

optionally rolling-standardized over a window W .

3.3 Layered Granger and VAR

We run block-Granger tests [10] in small VARs [17] with BIC-selected order (fixed-lag variants for robustness). We report F , p ,



Artifacts: logs/CSVs/PNGs under output/run_20250808_221301

Figure 1: End-to-end pipeline: factor construction → layered causality (A/B/C) and interpretable VAR/HAR-X → leakage-safe ML evaluation.

and BH-FDR q . Two compact VARs are used for interpretation: (i) a “main” block (LV + two vol-PCs + target); (ii) a vol-only block (vol-PCs + target), with orthogonalized IRFs and FEVDs plus Ljung–Box $Q(10)$ checks. We implement block-Granger tests in small VARs (order by BIC, with fixed-lag variants for robustness) and report the F-statistic, p -value, and Benjamini–Hochberg FDR q for each layer.

3.4 HAR-X with HAC

Following [8], we regress a market risk target y_t (our cross-sectional crowding or RV variants) on daily/weekly/monthly averages of volatility PCs:

$$y_t = \beta_0 + \beta_d \bar{v}_{t-1:t} + \beta_w \bar{v}_{t-5:t} + \beta_m \bar{v}_{t-22:t} + \varepsilon_t, \quad (1)$$

where $\bar{v}_{t-a:t}$ denotes the mean of vol-PC regressors over the indicated window. Inference uses Newey–West HAC standard errors.

3.5 ML Protocol (Leakage-Safe)

We construct an H -day risk index by blending short-horizon dispersion in features with structural shocks extracted from VARs. For $H=10$,

$$\text{risk_idx}_H(t) = \frac{1}{H} \sum_{h=1}^H \left(\sigma_{t-h+1}^{(\text{feat})} + |\varepsilon_{t-h+1}^{(\text{struct})}| \right), \quad (2)$$

where $\sigma^{(\text{feat})}$ is a rolling standard deviation of selected inputs and $\varepsilon^{(\text{struct})}$ are rolling mean absolute structural shocks. We run chronological splits (70%/15%/15% train/valid/test) with uniformly lagged features (+1 day) to ensure “use today to forecast $t+H$ ”. Models are XGBoost [6] with early stopping; we tune only on validation. The classification threshold is *chosen on the validation set* to maximize F1,

$$\hat{\tau} \in \arg \max_{\tau} \text{F1}(\text{valid}; \hat{p}(x) \geq \tau), \quad (3)$$

then *frozen* for the test set (positives correspond to the top 15% risk regime). SHAP values [13] are computed on the fitted booster for attribution; full predictions/curves reside under output/run_20250808_221301.

4 Experiments

We use the latest run directory output/run_20250808_221301 and robustness folder output/robust_output/compare_20251001_013842.

Full tables/CSVs are exported there; we include only the most probative figures below [12, 16, 18].

Key findings *Layer A*: 25/35 block-Granger tests are significant at $p < .05$ with BH-FDR control; liquidity/volatility of BNB, XEM, and YFI lead their own returns, while returns Granger-cause residual vol/turnover for most cores.

Layer B: 5/15 PC-to-PC links are significant; examples include pcLV → returns_PC3 and pcRET → {amihud_PC1, turnover_PC1, garch_vol_PC3, park_vol_PC1}.

Layer C: the raw market cross-sectional crowding target mkt_xsec_vol_12 is significantly predicted by volatility PCs at lag 3 ($p=0.0146$); standardized or leave- k -out variants are not significant in the latest run.

ML: the risk-index regressor attains test $R^2=0.53$; the classifier reaches ROC-AUC 0.74 and PR-AUC 0.47, using a threshold tuned only on validation and frozen on test.

Baselines: persistence-based regressions (AR/HAR-X) nearly saturate level prediction ($R^2 \approx 0.998$), while in classification logistic regression achieves a higher ROC-AUC (~ 0.90) but lower PR-AUC (~ 0.44); our leakage-safe XGBoost instead delivers the best PR-AUC (0.47–0.52 across RS windows), which is the more informative measure under imbalance and demonstrates its superior early-warning ability.

Table 1: Task & Metric & Best Model (Test Value)

Regression	R^2 (test)	AR(H): ~ 0.998
	MSE (test)	AR(H): ~ 1.41
Classification	ROC-AUC (test)	Logit: ~ 0.899
	PR-AUC (test)	XGB: 0.522 (RS252)
	F1 (test)	Logit: ~ 0.52
	Accuracy (test)	Logit: ~ 0.90

Layer A and B.

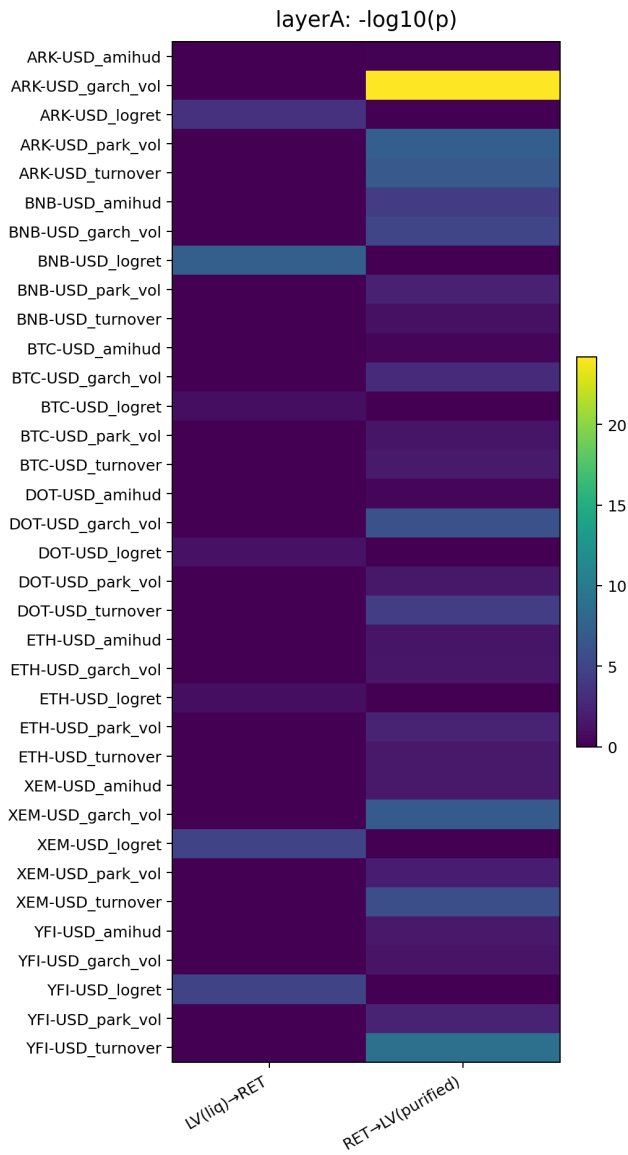


Figure 2: Layer A heatmap ($-\log_{10} p$). File: output/run_20250808_221301/heatmap_layerA.png.

Layer C robustness.

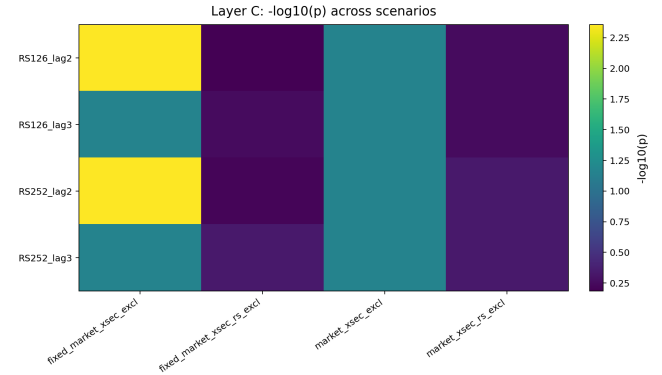


Figure 3: Layer C robustness across RS windows and fixed lags ($-\log_{10} p$). File: output/robust_output/compare_20251001_013842/robust_summary_layerC_heatmap.png.

VAR interpretation.

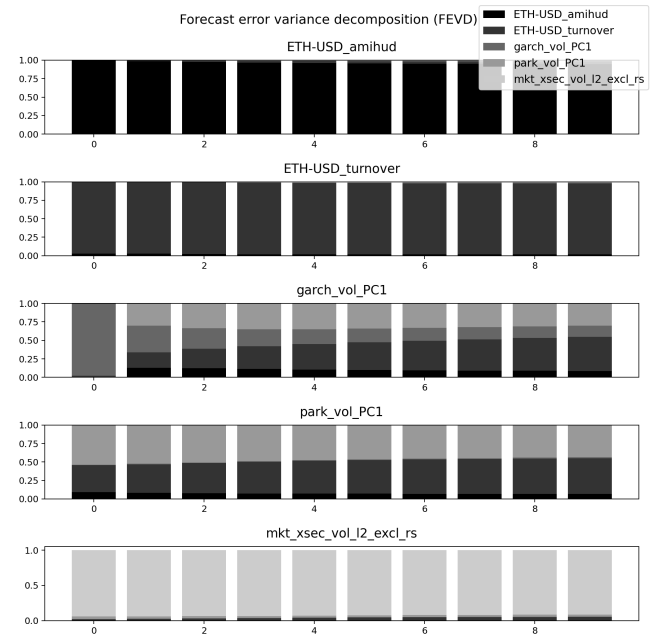


Figure 4: VAR (main) FEVD. File: output/run_20250808_221301/var_main_fevd.png.

ML evaluation (classification).

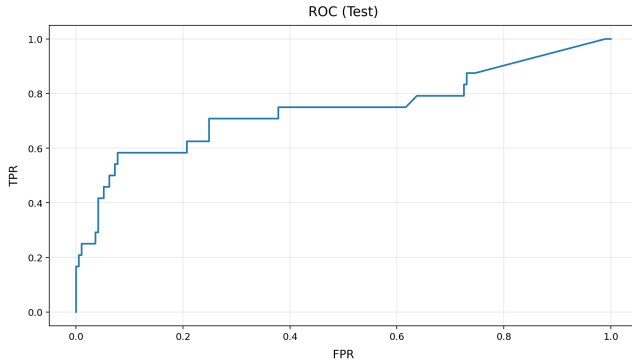


Figure 5: Test ROC curve (fixed threshold chosen on validation). File: output/run_20250808_221301/c1s_test_roc_curve.png.

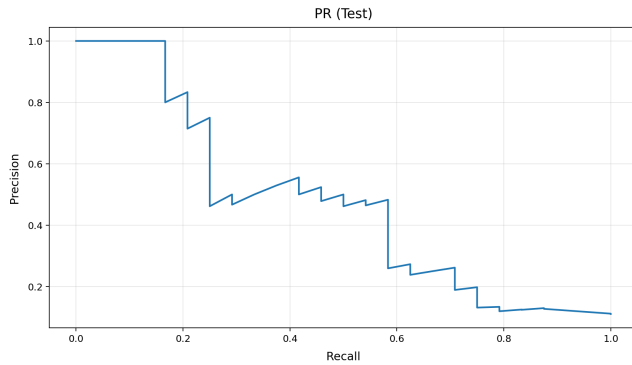


Figure 6: Test PR curve (fixed threshold chosen on validation). File: output/run_20250808_221301/c1s_test_pr_curve.png.

Baseline comparison. Under class imbalance (positives \approx top 15%), PR-AUC is the primary discriminator. While a calibrated Logit can post a high ROC-AUC (near 0.90), our XGBoost achieves a higher PR-AUC (0.47 vs. \sim 0.44), reflecting earlier concentration of true positives at actionable recall. We therefore emphasize PR-AUC and F1 at the validation-chosen, test-frozen threshold; full per-window metrics are in the artifacts.

Compact Layer C table.

Table 2: Layer C robustness (p-values; bold = significant at $q < 0.05$).

RS	Lag	Target	p-value	Sig.
126	2	Fixed/raw	0.004	✓
126	2	Fixed/RS	0.655	
126	3	Fixed/raw	0.070	
126	3	Fixed/RS	0.567	
252	2	Fixed/raw	0.004	✓
252	2	Fixed/RS	0.612	
252	3	Fixed/raw	0.070	
252	3	Fixed/RS	0.462	

5 Discussion and Limitations

Layer A shows LV/volatility (BNB, XEM, YFI) Granger-causing returns, while returns drive residual vol/turnover. Layer B links a non-market returns PC to vol-PCs. Layer C shows vol-PCs leading our cross-sectional crowding target at short lags. Limitations: modest sample length; sensitivity to RS-window in Layer C; potential structural breaks [1, 11]. We therefore provide robustness grids, alternative targets (RS vs. raw; leave- k -out), baselines and DM/CI comparisons in the artifacts.

Reproducibility. All results are fully reproducible from the artifact folder output/run_20250808_221301: we fix chronological splits and random seeds, export config.json and pipeline.log, and release the aligned CSVs and figure scripts that regenerate every table and plot.

6 Ethics

Risk forecasts can influence capital allocation; misuse may amplify herding. We export thresholds/diagnostics/SHAP for transparency and position this as an early-warning tool, not a trading recommendation.

References

- [1] Ismail Adelopo and Xiaojun Luo. 2025. Interconnectedness Among Cryptocurrencies and Financial Markets: A Systematic Literature Review. *Digital Finance* 5, 1 (2025), 61–101. doi:10.1007/s42521-025-00155-2
- [2] Yakov Amihud. 2002. Illiquidity and Stock Returns: Cross-section and Time-series Effects. *Journal of Financial Markets* 5, 1 (2002), 31–56. doi:10.1016/S1386-4181(01)00024-6
- [3] Jozef Baruník and Tomáš Křehlík. 2018. Measuring the Frequency Dynamics of Financial Connectedness and Systemic Risk. *Journal of Financial Econometrics* 16, 2 (2018), 271–296. doi:10.1093/jjfinec/nby001
- [4] Tim Bollerslev. 1986. Generalized Autoregressive Conditional Heteroskedasticity. *Journal of Econometrics* 31, 3 (1986), 307–327. doi:10.1016/0304-4076(86)90063-1
- [5] Sergey Brin and Lawrence Page. 1998. The Anatomy of a Large-scale Hypertextual Web Search Engine. *Computer Networks and ISDN Systems* 30, 1–7 (1998), 107–117.
- [6] Tianqi Chen and Carlos Guestrin. 2016. XGBoost: A Scalable Tree Boosting System. In *Proceedings of the 22nd ACM SIGKDD International Conference on Knowledge Discovery and Data Mining*. ACM, 785–794. doi:10.1145/2939672.2939785
- [7] Tarun Chordia, Richard Roll, and Avanidhar Subrahmanyam. 2000. Commonality in Liquidity. *Journal of Financial Economics* 56, 1 (2000), 3–28. doi:10.1016/S0304-405X(99)00057-4
- [8] Fulvio Corsi. 2009. A Simple Approximate Long-Memory Model of Realized Volatility. *Journal of Financial Econometrics* 7, 2 (2009), 174–196. doi:10.1093/jjfinec/nbp001
- [9] Francis X. Diebold and Kamil Yilmaz. 2012. Better to Give Than to Receive: Predictive Directional Measurement of Volatility Spillovers. *International Journal of Forecasting* 28, 1 (2012), 57–66. doi:10.1016/j.ijforecast.2011.02.006
- [10] C. W. J. Granger. 1969. Investigating Causal Relations by Econometric Models and Cross-spectral Methods. *Econometrica* 37, 3 (1969), 424–438. doi:10.2307/1912791
- [11] Mudassar Hasan, Muhammad Abubakr Naeem, Muhammad Arif, Syed Jawad Hussain Shahzad, and Xuan Vinh Vo. 2022. Liquidity Connectedness in Cryptocurrency Market. *Financial Innovation* 8, 1 (2022), 3. doi:10.1186/s40854-021-00308-3
- [12] Yujun Liu, Zhongfei Li, Ramzi Nekhili, and Jahangir Sultan. 2023. Forecasting Cryptocurrency Returns with Machine Learning. *Research in International Business and Finance* 64 (2023), 101905. doi:10.1016/j.ribaf.2023.101905
- [13] Scott M. Lundberg and Su-In Lee. 2017. A Unified Approach to Interpreting Model Predictions. In *Advances in Neural Information Processing Systems*. Curran Associates, Inc., Long Beach, CA, USA, 4765–4774. doi:10.48550/arXiv.1705.07874
- [14] Whitney K. Newey and Kenneth D. West. 1987. A Simple, Positive Semi-definite, Heteroskedasticity and Autocorrelation Consistent Covariance Matrix. *Econometrica* 55, 3 (1987), 703–708. doi:10.2307/1913610
- [15] Michael Parkinson. 1980. The Extreme Value Method for Estimating the Variance of the Rate of Return. *Journal of Business* 53, 1 (1980), 61–65. doi:10.1086/296071
- [16] Yue Qiu, Yifan Wang, and Tian Xie. 2021. Forecasting Bitcoin Realized Volatility by Measuring the Spillover Effect Among Cryptocurrencies. *Economics Letters* 208 (2021), 110092. doi:10.1016/j.econlet.2021.110092
- [17] Christopher A. Sims. 1980. Macroeconomics and Reality. *Econometrica* 48, 1 (1980), 1–48. doi:10.2307/1912017
- [18] Yijun Wang, Galina Andreeva, and Belén Martín-Barragán. 2023. Machine Learning Approaches to Forecasting Cryptocurrency Volatility: Considering Internal and External Determinants. *International Review of Financial Analysis* 90 (2023), 102914. doi:10.1016/j.irfa.2023.102914